Model-based Clinical Assist System for Cardiac Ablation

Yutong Wu
wuyt@shanghaitech.edu.cn
ShanghaiTech University

Renzhi Tang
tangrz@shanghaitech.edu.cn
ShanghaiTech University

Eunsuk Kang
eunsukk@andrew.cmu.edu
Carnegie Mellon University

Zhihao Jiang
jiangzhh@shanghaitech.edu.cn
ShanghaiTech University and Shanghai Engineering Research Center of Intelligent Vision and Imaging

ABSTRACT

Cardiac Ablation is an effective treatment of arrhythmia in which physicians terminate fast heart rate by transecting abnormal electrical conduction pathways in the heart with RF energy. During the procedure, physicians diagnose the condition of the heart and locate ablation sites by analyzing electrical signals sensed by catheters inserted into the heart. Due to the limited observation of the patient's heart, there may exist multiple heart conditions that can explain historical observations, causing ambiguities in the patient's heart condition. During the procedure, physicians have to visualize and continuously update these suspected heart conditions in their mind, causing heavy mental burden on the physicians. In this paper, cardiac electrophysiology is formalized using a physiological model of the heart, such that the diagnosis problem during cardiac ablation can be formalized as parameter identification and state estimation problems with the heart model. We then propose a model-based clinical assist system which partially solves the diagnosis problem during cardiac ablation. The system enumerates suspected heart conditions by creating "digital twins" of the patient's heart with heart models. The heart models are used to represent and visualize suspected heart conditions, and are systematically updated and removed with new information during the ablation procedure. The system provides more rigorous and intuitive interpretation of current understanding of the patient's heart, and improves the accuracy and efficiency of cardiac ablation procedures by relieving the physicians from demanding low-level reasoning.

KEYWORDS

Digital Twin, System Identification, Knowledge Representation

ACM Reference Format:
Yutong Wu, Renzhi Tang, Eunsuk Kang, and Zhihao Jiang. 2021. Model-based Clinical Assist System for Cardiac Ablation. In *ACM/IEEE 12th International Conference on Cyber-Physical Systems (with CPS-IoT Week 2021) (ICCPS '21), May 19–21, 2021, Nashville, TN, USA.* ACM, New York, NY, USA, 11 pages. https://doi.org/10.1145/3450267.3450539

ICCPS '21, May 19–21, 2021, Nashville, TN, USA

ACM ISBN 978-1-4503-8353-0/21/05…$15.00
https://doi.org/10.1145/3450267.3450539

1 INTRODUCTION

Coordinated contractions of our heart are essential to our health, and are governed by electrical activities within the heart. Electric excitation can develop and circulate around structurally-defined or undefined circuits, resulting in abnormally fast heart rate. This mechanism is referred to as reentry, and is the dominant cause of tachycardia [17]. Depending on the locations of the reentry behavior, tachycardia can cause serious consequences like stroke [4], and even death [15]. Clinical studies suggest rising prevalence and incidence of tachycardia, with increases in overall burden and mortality all over the world [5].

Cardiac ablation has been an effective treatment of tachycardia. By inserting catheters through the veins into the heart (Fig. 1.(b)), physicians can observe electrical activities within the heart, which are referred to as the *Electrogram signals* (EGMs) (Fig. 1.(c)). Catheter locations within the heart can be obtained from *fluroscopic images* as well as more advanced *Electro-Anatomic Mapping* (EAM) system[3]. Based on these spatial-temporal observations, physicians infer the current heart condition of the patient, and then identify and "kill" heart tissue with anomalies (i.e. reentry circuits) using RF energy [13]. Cardiac ablation can effectively terminate structural reentry tachycardia [12], and has demonstrated better outcome than anti-arrhythmic drugs in non-structural tachycardia like Atrial Fibrillation [16].

Typical cardiac ablation procedures range from 3-6 hours, with majority of time spent on diagnosing the heart condition of the patient [13]. Due to the minimally invasive nature of the cardiac ablation procedure, the number of catheters inside the heart is very limited. Patients with the same disease mechanism may also exhibit different observable behaviors due to the large variability among patients. Therefore, the patient's heart can be viewed as a *partially-observable system* with unknown parameters, which means at a particular time, there exists multiple heart conditions that can explain historical observations. In most of the clinical cases that require cardiac ablation procedure, suspected heart conditions cannot be distinguished via passive observations alone. Physicians need to deliver electrical pacing sequences from catheters to the heart, so that previously indistinguishable heart conditions will exhibit different observations. This process is referred to as *Electro-Physiological (EP) Testing*. During EP testing, physicians iteratively perform the following tasks until an unambiguous diagnosis is achieved:

(1) Identify all possible heart conditions that can explain historical EGM observations

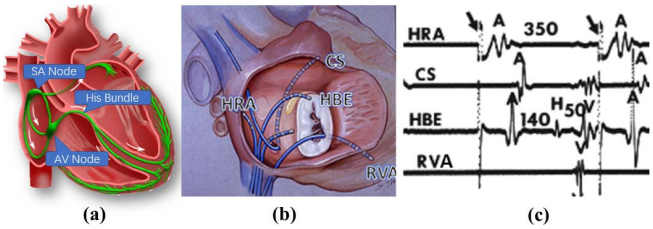

Figure 1: (a) Electrical conduction system of the heart; (b) Common catheter configuration; (c) Example of EGMs observed from corresponding channels [13].

(2) Eliminate heart conditions if information in these heart conditions conflicts with information in new EGM observations
(3) Update remaining heart conditions with information obtained from new observations
(4) Identify pacing sequences that can distinguish suspected heart conditions

The amount of reasoning and calculations involved in these tasks place heavy mental burden on physicians. Some of these reasoning become subconscious as physicians gain experience, which requires years of practice. As the result, the experience level of physicians affects not only the time consumption, but also the chances of clinical complications during the procedure [7]. A more experienced physician takes less time and makes fewer mistakes than a less experienced one. With increasing number of cardiac ablation procedures performed every year [14], there is need to reduce physicians' mental load, bridge the experience gap among physicians with different experience level, and improve the overall efficiency of the ablation procedure.

As discussed above, the physician maintains "models" of the patient's heart in their mind. The parameters and state of the "models" are constantly updated with new information from observations to reflect the actual heart condition of the patient. The process aligns with the *Digital Twin* concept used in various industries like manufacturing [8]. In this project, we propose a model-based clinical assist system that can reduce physician workload during cardiac ablation procedure. Digital twins of the patient's heart are created and updated based on observations to explicitly represent and visualize the ambiguities of heart conditions during the procedure, which provide rigorous yet interpretable guidance to the physicians. The overview diagram of the system is shown in Fig. 2. The system runs in parallel with the current cardiac ablation procedure setup. The real-time inputs to the system include: 1) sensed EGM signals; 2) pacing sequences delivered to the patient; and 3) catheter locations sensed by the EAM system. The output of the system includes: 1) suspected heart conditions and their interpretable visualizations; and 2) suggestion on pacing sequences that can distinguish suspected heart conditions.

In this paper, we focus on identifying suspected heart conditions during cardiac ablation procedure, which is a prerequisite for pacing sequence suggestion. In our clinical assist system, suspected heart conditions of the patient are represented by digital twins of the patient's heart, which are physiological models of the heart. The state and parameters of the heart models are incrementally updated

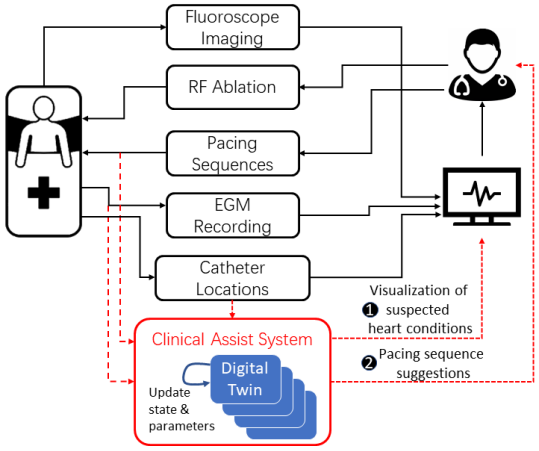

Figure 2: System Overview

to reflect the current understanding of the patient's heart. The state and parameters of the heart models are clinically-relevant, therefore the digital twins can provide interpretable visualization of the patient's heart condition during cardiac ablation. Ambiguities arisen during the procedure are enumerated by separate digital twins, and digital twins that have conflicts with information obtained from new observations are eliminated.

At the beginning of a cardiac ablation procedure, a set of heart models for different arrhythmia with unknown parameters are provided as the input to our clinical assist system, which reflect prior knowledge on the patient's heart condition. The clinical assist system performs the following tasks iteratively for every new observation during cardiac ablation:

(1) Enumerate all possible heart models in terms of their state and parameters, such that the simulation of the heart models can explain historical observations.
(2) If information from the new observation conflict with information in a heart model, the heart model is eliminated
(3) Update the state and parameters of the heart models based on the new observation

These tasks align and complement with the physicians' activities during cardiac ablation, which can reduce physicians' effort during diagnosis. The digital twins rigorously represent uncertainties during cardiac ablation procedures, which helps the physicians to achieve correct diagnosis with higher efficiency and accuracy. The system can significantly reduce the mental load of the physicians during cardiac ablation procedures. It can also bridge the experience gap among physicians so that cardiac ablation procedure can be more accessible.

The contributions of this paper is 3-folds: 1) We formalized the diagnosis problem during cardiac ablation procedure as creating digital twins of the patient's heart, which involves identifying the parameters and estimating the state of the patient's heart; 2) We proposed using interpretable heart models to represent uncertainties and ambiguities in heart conditions during ablation procedure; and 3) We developed a clinical assist system that can partially solve

the diagnosis problem during cardiac ablation by enumerating, eliminating and updating digital twins of the patient's heart.

The rest of the paper is arranged as follows: In Section 2, we provide background knowledge on cardiac ablation procedure, with focus on the sources of uncertainties and the challenges of correct diagnosis. In Section 3, we introduce the heart model structure and formally define the diagnosis problem in terms of the heart model during cardiac ablation procedure. In Section 4, we propose a partial solution for the diagnosis problem based on clinical knowledge. In Section 5, we use a clinical case study to demonstrate the functionalities of our system. In Section 6, we discuss other clinical and research efforts to improve efficiency and accuracy of cardiac ablation procedures. We then end the paper with discussions and future work.

2 CARDIAC ABLATION BASICS

In this section, we briefly introduce the domain knowledge required to understand cardiac ablation. These knowledge will be encoded into our clinical assist system in forms of heart models and physiological rules, and will be used during identification of suspected heart conditions during cardiac ablation.

2.1 Cardiac Electro-Physiology (EP)

The coordinated contractions of the heart are governed by electrical activities inside the heart. Heart tissue can be *depolarized* by electrical stimulus, which results in voltage change outside of the tissue. The increased voltage caused by depolarization will then depolarize nearby tissue, causing propagation of electrical signals with delays.

Tissue with different timing parameters form the electrical conduction system of the heart, which is shown in Fig. 1.(a). In a healthy heart, electrical depolarization starts from the SA node, which is a structure that can depolarize itself. The signal then propagates throughout both atria, causing atrial contraction and pump blood into the ventricles. After some delay at the AV node, the signal then propagates throughout the ventricles and pump blood to the whole body. This healthy heart rhythm is referred to as the *Normal Sinus Rhythm* (NSR).

The timing of these electrical activities ensures hemodeynmics with efficient blood supply, and are essential to our health. Derangements from NSR are referred to as *arrhythmia*, which can cause serious health problems. Abnormally fast heart rate is referred to as *tachycardia*. Anomalies that can cause arrhythmia include: 1) additional pathways, which can form conduction circles within the heart, causing dangerous reentry tachycardia; 2) degeneration of heart tissue, which can affect its refractory period, conduction delay or rate of self-depolarization; and 3) the combination of the first two. Therefore, diagnosis of the heart condition includes identifying 1) the structure of the electrical conduction network, and 2) the parameters of key heart tissue.

2.2 Electrophysiological (EP) Testing

EP testing is the early stage in cardiac ablation procedure in which physicians gain understanding of the condition of the patient's heart and localize ablation sites. By inserting catheters with electrodes into the heart from the vein in the groin area of the patient, physicians can observe local electrical activities at various locations of the heart.

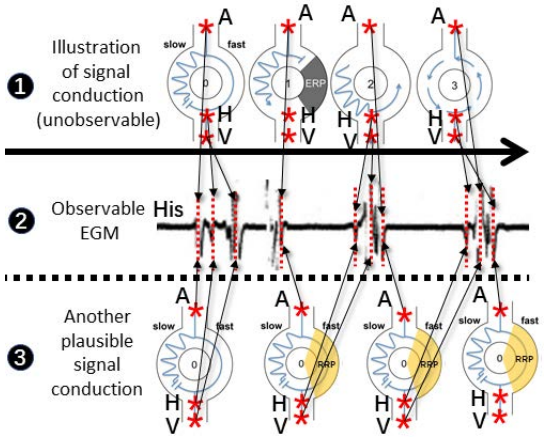

Figure 3: 1) Illustration of electrical conduction within the heart over time; 2) Corresponding EGM signal from the His catheter; 3) Another signal conduction pattern that can explain the same EGM observation

Fig. 1.(b) shows a commonly used configuration for stationary catheters. Besides the stationary catheters, moving catheters are also used to monitor local electrical activities at locations of interest. Electrical activities observed from these catheters are referred to as *electrograms* (EGMs). Each "impulse" represents either a depolarization of local tissue (near-field) or electrical reflection from strong electrical activities including pacing or heart chamber contractions (far-field).

These catheters can only capture local and partial information about the heart, which may cause ambiguities on the state of the patient's heart. These ambiguities and uncertainties reflect in the EGMs as well, which makes it difficult to interpret and extract information from. In EP related textbooks, annotations are provided on EGMs to provide more intuitive interpretation. These annotations include source and/or properties of electrical signals, as well as key intervals between signals (Fig. 1.(c)). However, during the procedure there are no real-time EGM annotations. Correct annotation of EGM signals is an indication of correct diagnosis of current heart condition.

Fig. 3 demonstrated a clinical case in which observable EGM can be explained by multiple heart conditions. Row 2 shows the His EGM of a patient, and the red dotted lines mark the impulses. Row 1 demonstrates the conduction trajectory of electrical signals within the patient's heart, and the red stars mark the tissue that are being observed by the His catheter. The black arrows illustrate how impulses in His EGM correspond to observable tissue depolarizations at different time. Row 3 shows another heart condition that can also explain the same EGM sequence. The patterns of electrical conduction are different in Row 1 and 3, but are not distinguishable given the His EGM in Row 2. During the ablation procedure, physicians are required to consider all plausible heart conditions that can explain historical observations, and update them with information gathered from new observations. As the complexity of

the heart condition increases, the number of plausible heart conditions increases rapidly, which makes tracking every heart condition infeasible, causing inaccurate and inefficient diagnosis.

3 FORMALIZING THE DIAGNOSIS PHRASE OF CARDIAC ABLATION PROCEDURE

The diagnosis problem of cardiac ablation procedure has been extensively discussed in clinical literature like [13]. However, these knowledge are implicitly described in terms of case studies. In this section, we formalize cardiac electrophysiology using physiological model of the heart, the diagnosis problem during cardiac ablation can therefore be formulated as parameter identification and state estimation problem on the heart model.

3.1 Modeling Cardiac Electrophysiology

Physicians' Conceptual Model of Cardiac Arrhythmia

In clinical cardiac electro-physiology, physicians have developed a conceptual model h^C to describe electrical activities within the heart (Fig. 4). As the electrical activities of most heart tissue are not observable, physicians only take into account key anatomical and functional structures of the heart during analysis. The remaining heart tissue are abstracted as conduction pathways among these key tissue. The heart is then viewed as an electrical conduction network in which electrical signals are generated and traverse throughout. As shown in Fig. 4, the reentry circuit formed around scar tissue in the real heart h^R is abstracted as a conduction loop in the conceptual model h^C.

The conceptual model h^C represents domain knowledge needed during cardiac ablation, and is essential for an interpretable clinical assist system. However, the conceptual model is not formally defined, and is mostly illustrated in clinical literature in terms of case studies.

Formalizing the Conceptual Model h^C

In [11], Jiang et.al proposed the Virtual Heart Model (VHM), which is an EP heart model framework for implantable cardiac device validation [10]. The structure of the conceptual model h^C, which represents the electrical conduction network of the heart, is abstracted as an undirected graph in VHM:

$$\gamma = \langle V, E \rangle$$

Each $v \in V$ is represented by a node automaton, which models the tissue's behaviors in generation and blocking of electrical signals. Each edge $e \in E$ is represented by a path automaton, which models the conduction of electrical signals among heart tissue (Fig. 4). The node and path automata are connected via synchronization events, such that if there exists $e_1 = (v_1, v_2) \in E$, we have $v_1.Act\_path \Rightarrow e_1.Act\_path\_1$, $v_2.Act\_path \Rightarrow e_1.Act\_path\_2$, $e_1.Act\_node\_1 \Rightarrow v_1.Act\_node$, $e_1.Act\_node\_2 \Rightarrow v_2.Act\_node$, in which $\Rightarrow$ is the mapping of synchronization events.

Each node and path automaton is a timed automaton [1], which is a tuple $\langle Q, Q_0, \Sigma, X, inv, \rightarrow \rangle$ where:

- Q is a finite set of locations
- $Q_0 \in Q$ is the set of initial locations
- Σ is the set of events
- X is the set of clocks

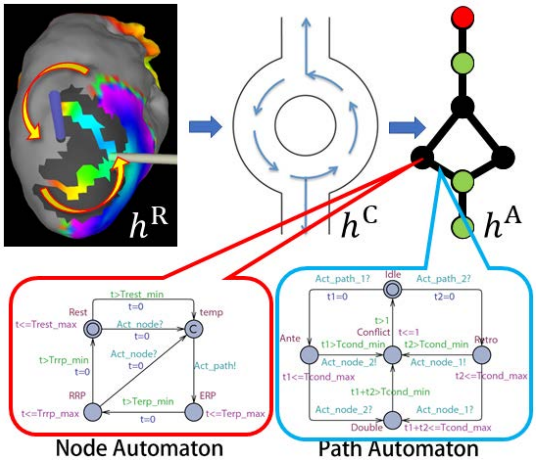

Figure 4: The conceptual model h^C abstracts the observable behaviors of the real heart h^R, and the heart model h^A formalizes h^C as a network of timed automata. Node automata model generation and blocking of electrical signals, and path automata model conduction delay between nodes.

- inv is the set of invariants for clock constraints at each location
- $\rightarrow$ is the set of transitions, each of which is a tuple $\langle q, \sigma, g, \lambda, q' \rangle$ which consists of a source location q, an event $\sigma \in \Sigma$, guard as clock constraints g, λ as a set of clocks to be reset and the target location q'

Each heart model is a combined timed automaton which is the product of all node and path automata $h^A = \prod_{i=1}^{N} v_i \times \prod_{j=1}^{M} e_j$, in which $v_i \in V, e_j \in E$. The parameters of a heart model include:

- Topology of the electrical conduction network γ
- The amount of time that an automaton can stay in different locations, the minimum and maximum of which are determined by the invariant inv of the location and the guard g on the out-going edge from the location. Each node automaton has three parameters $\{TERP, TRRP, TRest\}$, representing the blocking periods and the generation period. Each path automaton has one parameter $\{TCond\}$, representing the conduction delay between two nodes.

By adjusting the parameters of h^A, the heart model has demonstrated its capability to model electrical behaviors of various heart conditions [11], which makes it a validated abstraction and formalization of the conceptual model h^C.

Interface of the Heart Model During Cardiac Ablation

During cardiac ablation, catheters inserted into the patient's heart can observe electrical activities of nearby tissue. Physicians can also deliver external pacing through the catheters. In the heart model, these tissue are represented by the node automata of a subset of the vertices $V^O \subset V$ (Green circles in h^A in Fig. 4). The $Act\_path \in \Sigma$ events from V^O can be observed by the corresponding catheter, and pacing signals can trigger $Act\_node \in \Sigma$ events of corresponding node automata. Within the heart model, some heart tissue $V^A \subset V$

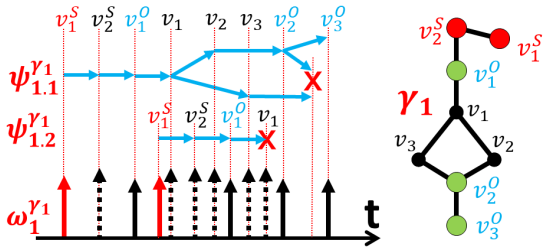

Figure 5: Two traversal trees $\psi_{1.1}^{\gamma_1}$ and $\psi_{1.2}^{\gamma_1}$ on topology γ_1 map to a temporal trace ω^{γ_1}

(Red circles in h^A in Fig. 4) can generate $Act\_path \in \Sigma$ events autonomously, together with external pacing, $V^S = V^A \cup V^O$ are the possible sources of electrical events within the heart.

3.2 From Mechanism to Observation

The simulation of heart model h^A can be used to explain how electrical signals traverse the heart and generate EGM observations.

Electrical Propagation Within the Heart

Electrical activities of the heart originate from $v^S \in V^S$ and propagate throughout the heart. Assume a sequence of m stimuli S is applied to a heart model with topology γ:

$$S = (s_i^j | i \in [1, m], v_j^S \in V^S)$$

This process can be represented by creating a set of graph traversal on γ for each s_i^j. Depending on the state of the heart, a stimuli sequence S can have different traversal patterns. We define the pth set of *traversal trees* for the stimuli sequence S on graph γ as:

$$\Psi_p^\gamma = (\psi_{p.1}^\gamma, \psi_{p.2}^\gamma \dots \psi_{p.m}^\gamma)$$

in which $\psi_{p.m}^\gamma$ is the traversal tree initiated by the mth stimulus s_m^j with v_j^S as root:

$$\psi_{p.m}^\gamma = \langle V^\psi, E^\psi, T^\psi \rangle$$

in which $V^\psi \subseteq V$ are the reachable vertices from v_j^S, and $E^\psi \subseteq E$ are the edges if both vertices connected by the edge are reachable from v_j^S. T^ψ contains the global time when each $v^\psi \in V^\psi$ is activated. If the graph is acyclic and connected, $\psi_{p.m}^\gamma$ has the same structure as γ with v_j^S as root, and each vertex can be visited once. However, if there exists loops in γ, vertices on the loops may be visited multiple times in the traversal tree, which corresponds to the reentry mechanism.

Temporal Trace of Electrical Propagation

With a set of traversal trees Ψ^γ, we define:

$$C(\Psi^\gamma) = \omega^\gamma$$

to extract temporal information from a spatial-temporal traversal tree. $\omega^\gamma = (v_1, v_2 \dots v_n), v_i \in V$ is a *temporal trace* in which vertices visited in γ are listed in chronological order $(T^\psi(v_j) <= T^\psi(v_{j+1}))$.

Fig. 5 demonstrates how a set of traversal tree $\Psi_1^{\gamma_1}$ on heart topology γ_1 maps to a temporal trace $\omega_1^{\gamma_1}$. Both $\psi_{1.1}^{\gamma_1}$ and $\psi_{1.2}^{\gamma_1}$ start from external stimulus applied to v_1^S. In $\psi_{1.1}^{\gamma_1}$, the conduction delay in $(v_1, v_2) + (v_2, v_2^O)$ is shorter than the one in $(v_1, v_3) + (v_3, v_2^O)$. Therefore the signal conducted through $(v_1, v_2) + (v_2, v_2^O)$ reached v_2^O first and started conducting through the edge (v_2^O, v_3). At the same time, another signal is conducting through the same edge from the opposite direction (v_3, v_2^O), causing conflict and conduction cancellation (marker x in Fig. 5).

$\psi_{1.2}^{\gamma_1}$ started shortly after $\psi_{1.1}^{\gamma_1}$ before all heart tissue in γ_1 has finished their refractory periods. Therefore the signal could only conduct to v_1 before blocked at v_1. Tissue activations in both $\psi_{1.1}^{\gamma_1}$ and $\psi_{1.2}^{\gamma_1}$ are then mapped to ω^{γ_1} and lost their spatial information.

Mapping to Observable EGMs

During cardiac ablation, electrical activities of the patient's heart can be observed via EGM signals. These observation O contains signals from different channels:

$$c \in \{HRA, CS, His, RVA \dots\}$$

which correspond to different catheters inside the heart. Each channel observes a sequence of impulses over time

$$O^c = (\sigma_1^c, \sigma_2^c \dots \sigma_n^c), i \in \mathbb{N}$$

Each impulse represents depolarization of heart tissue V^O in the heart model. Each channel c can observe a subset of $V_c^O \subset V^O$. We define mapping $B_c(\omega)$ which extracts the vertices observable by channel c from a trace ω^γ:

$$B_c(\omega^\gamma) = \alpha^c$$

in which $\alpha^c = (v_1, v_2 \dots v_n), v_i \in V_c^O \cup V^S$. The correspondence between an impulse in EGMs and an observable heart tissue depolarization is referred to as *annotation*:

$$A_c(\sigma^c) = v, v \in V_c^O \cup V^S$$

The annotation mapping can also be applied to observation traces:

$$A_c(O^c) = \alpha^c$$

Therefore α^c is referred to as an *annotation trace* for channel c.

Fig. 6 demonstrates how multiple traversal tree sets can explain the same EGM observation. O^{His} is the EGM signal observed from the His catheter with seven observable impulses as well as two external stimuli applied to the heart at tissue v_1^S. There are two suspected heart topologies γ_1 and γ_2. For γ_1 there are two plausible traversal patterns represented by two sets of traversal trees $\Psi_1^{\gamma_1}$ and $\Psi_2^{\gamma_1}$, which are shown in Fig. 6 (a) and (b). In $\psi_{1.2}^{\gamma_1}$ of $\Psi_1^{\gamma_1}$, the second stimulus triggered reentry behavior around the loop inside γ_1, while in $\Psi_2^{\gamma_1}$, the second stimulus triggered the same traversal pattern as the first stimulus. As the result, the two traversal tree sets have different number of traversal trees and annotations of O^{His}. The other topology γ_2 also has a set of traversal tree $\Psi_1^{\gamma_2}$ that can explain O^{His}, which cannot be ruled out with existing observations. The traversal trees are morphed along the topology for better visualization.

3.3 Diagnosis During Cardiac Ablation

During the diagnosis process of cardiac ablation, physicians need to acquire the following information regarding the patient's heart in order to achieve precise diagnosis: 1) Structure of the electrical conduction network, 2) Physiological parameters of key heart tissue, 3) How electrical signals traversed through the conduction network.

The diagnosis process during cardiac ablation can be formulated as creating *Digital Twins* of the patient's heart with the heart model

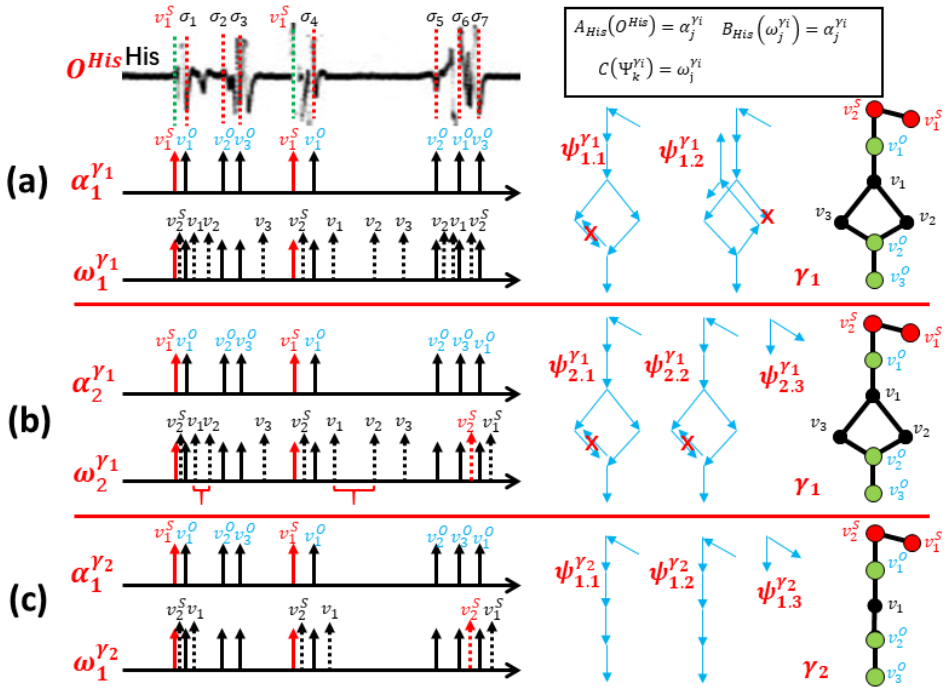

Figure 6: The same EGM observation can be explained by multiple traversal tree sets based on multiple heart topologies.

h^A, which include 1) identifying the parameters and 2) estimating the state of h^A.

Parameter Identification

Two categories of parameters of the heart model are estimated during cardiac ablation procedure:

(1) Topology γ: The topology of the electrical conduction network illustrates whether there exists abnormal pathways within the heart, which is a deciding factor for diagnosis. Before the procedure, physicians normally have a short list of suspected topologies based on prior diagnosis of the patient.
(2) Parameter range cp: Precise value of timing parameters of the heart model can rarely be determined during the procedure. However, linear constraints on the parameters can be obtained from EGM observations, which help the physicians to decide whether certain tissue is healthy.

State Estimation

Parameter identification only provides "static" information regarding the patient's heart, which is not enough for precise diagnosis. The traversal tree set Ψ^γ, which represents how an electrical signals traversed through the heart topology γ, visualizes the state sequence of h^A that can explain the observations, which can be very helpful during diagnosis.

Representing Ambiguities with Digital Twins

As the patient's heart is a partially-observable system with unknown parameters, there exist multiple traversal tree sets Ψ^γ that can explain historical observations during the procedure. Ambiguities come from, but not limiting to the following sources:

- State of the heart that are neither observable nor diagnosable
- The reliability of sensor reading (false-positives, false-negatives, overlapped events)
- The sources of electrical stimuli (internal, external)
- Limited sensor capability (events observed from the same channel are not distinguishable)

In this project, we represent the ambiguities using heart conditions, which are digital twins of the patient's heart. Assume there exists N suspected heart conditions that can explain the k observed events during the cardiac ablation procedure, we define *heart conditions* as the parameters and states of the timed automata model h^A:

$$h_i[k] = \langle \gamma, cp, \Psi^\gamma[k] \rangle, i \in N$$

The diagnosis of heart condition during cardiac ablation can be formally defined as identifying the heart conditions that can explain existing observations:

$$H^\gamma[k] = \{h_i^\gamma[k] | A_c^{-1}(B_c(C(h_i^\gamma[k].\Psi_i^\gamma[k]))) = O^c[1,k] \quad \forall \gamma \in \Gamma, \forall c \in C, \\ \wedge h_i^\gamma[k].cp \models (h_i^\gamma[k-1].cp \cup D)\} \quad (1)$$

Each heart condition $h_i^\gamma[k]$ contains traversal tree set $\Psi_i^\gamma[k]$ such that the temporal sequence $\omega_i = C(\Psi_i^\gamma[k])$ contains annotation trace $\alpha_i = B(\omega_i)$ that can map to the first k impulses in the EGM sequence $O^c[1,k] = A_c^{-1}(\alpha_i)$.

The parameters constraints of the heart condition $h_i^\gamma[k].cp$ should be consistent with parameter constraints before observing the kth impulse $h_i^\gamma[k-1].cp$, as well as domain knowledge D, which can also be specified as linear constraints on heart model parameters.

In the following section, we discuss the proposed clinical assist system which enumerates and represents the ambiguities with heart

conditions, while updating and eliminating heart conditions with information obtained from new observations.

4 CLINICAL ASSIST SYSTEM FOR CARDIAC ABLATION

In this section, we introduce our current implementation of the proposed clinical assist system, which automatically analyse EGM signals and visualize suspected heart conditions to the physicians during cardiac ablation.

We make the following assumptions in this preliminary work:

A1) The patient has anatomy-based arrhythmia (the heart topologies are static);

A2) Catheters are not moving (the locations of V^O and their topological relationship with other vertices are fixed);

A3) External stimuli are the only sources of electrical signals;

A4) All impulses reflect actual tissue depolarization and there are no missed impulses.

4.1 Overview of System Execution

The system is initialized with a set of suspected heart topologies Γ, which are chosen by the physicians before the procedure based on prior knowledge of the patient's condition. The set of V^S and V^O are identified in each γ based on the catheter configuration. The system starts when the first impulse σ_1^c is observed in EGM channel c, which occurred after the first stimulus $s_1^j \in S$ is applied to $v_j^S \in V^S$. The system first traverses all Γ from their corresponding v_j^S, until the first $v^O \in V_c^O$ is reached on every traversal paths, resulting in i traversal trees $\psi_{i.1}^{\gamma}[1]$ for i heart conditions $h_i^{\gamma}[1]$. The set of v^O corresponds to plausible annotations of σ_1^c. Each of the i traversal trees is created for each different v^O that can be first reached from s_1^j, in order to represent the ambiguities of $A_c(\sigma_1^c)$. Other sources of ambiguities are also represented by creating new heart conditions for each ambiguous condition.

Heart conditions are updated upon every new observable impulses. For instance, when new impulse σ_2^c is observed, the electrical conduction initiated by s_1^j is still traversing γ. This behavior is represented by extension of all traversal tree $\psi_{j.1}^{\gamma}[1]$ to the next reachable v^O in γ. For topologies γ without loops, which is a tree, the traversal terminates when all leaf vertices are reached.

New observations also provide information on heart model parameters in terms of linear constraints in cp. i.e. The sum of conduction delays of all edge e on the path between s_1^j and $A_c(\sigma_1^c)$ is equal to the interval between s_1^j and $A_c(\sigma_1^c)$ ($\sum e.Tcond = T(\sigma_1^c) - T(s_1^j)$). The newly inferred information cp_n should be incorporated into the updated heart model, which can be achieved by performing linear programming algorithm on $cp_n \cup h_i^{\gamma}[1].cp$. If there exists solutions, the constraints cp become "tighter", which reduces the uncertainty of heart model parameters. If there is no solution, the heart condition before update has faulty assumptions on the real heart condition, therefore should be eliminated from further consideration.

New stimulus s_k^j initializes new traversal trees $\psi_{m.k}^{\gamma}$ in γ. For an observation σ_i^c occurred after s_k^j, it is ambiguous whether σ_i^c is triggered by s_k^j or s_{k-1}^j. This ambiguity is also represented by separate heart conditions with traversal tree sets corresponding to the two scenarios. As discussed above, each heart condition $h_i^{\gamma}[k]$ creates one or more $h_j^{\gamma}[k+1]$ after each observation. The system maintains a set of *uncertainty trees* T^{γ} for each heart topology γ. The kth level of T^{γ} contains heart models $h_i^{\gamma}[k-1]$, and plausible annotations $annot_i$ for σ_{k-1}.

Example

Fig. 7 illustrates the evolution of two heart conditions after observing 7 impulses in the His channel. Two topologies γ_1 and γ_2 are considered before the procedure. After receiving $S1$ at HRA_A and observing σ_1^{His} in the His channel, traversal trees $\psi_{1.1}^{\gamma_1}[1]$ and $\psi_{1.1}^{\gamma_2}[1]$ are created for both topologies. With new observations σ_2^{His} and σ_3^{His} the traversal trees are extended to the next two possible v^O. When $S2$ and σ_4^{His} are observed, new traversal trees $\psi_{1.2}^{\gamma_1}[4]$ and $\psi_{1.2}^{\gamma_2}[4]$ are created. Since both $\psi_{1.1}^{\gamma_1}[3]$ and $\psi_{1.1}^{\gamma_2}[3]$ cannot be traversed further, there is no ambiguity that σ_4^{His} is triggered by $S2$.

When σ_5^{His} is observed, $\psi_{1.2}^{\gamma_2}[4]$ can only be extended to node His_H. However, from $\psi_{1.1}^{\gamma_1}[2]$ and $\psi_{1.1}^{\gamma_2}[2]$ we know the conduction delay from v^{His_A} to v^{His_H} in both topologies is equal to the interval between σ_1^{His} and σ_2^{His}. Interval between σ_4^{His} and σ_5^{His} is much longer, which conflict with historical information in $h_1^{\gamma_2}[4]$. Therefore heart model $h_1^{\gamma_2}[4]$ with traversal tree $\psi_{1.1}^{\gamma_2}[4]$ and $\psi_{1.2}^{\gamma_2}[4]$ is removed from further consideration. In γ_1 there exists another path from v^{His_A} to v^{His_H} so the longer delay can still be explained. Therefore $\psi_{1.2}^{\gamma_1}[4]$ is further traversed around the loop in γ_1 to explain $\sigma_5^{His}\sigma_6^{His}\sigma_7^{His}$, representing the reentry behavior. The uncertainty tree T^{γ_1} contains plausible heart conditions in each iteration. The letter on each vertex represent plausible annotations for each observation. The annotation sequence from the root of T^{γ_1} to a leaf vertex represent a plausible annotation sequence $A_{His}(O^{His})$ for the observation sequence O^{His}.

The system is implemented by Algorithm 1-3, which are shown in the Appendix. For each new impulse σ observed in EGM O, Algorithm 1 *AnalyzeEGM()* is called to enumerate and update heart conditions. *AnalyzeEGM()* calls Algorithm 2 *TpTraverseIter()*, which is a modified Breath-First Search (BFS) algorithm, to construct and update traversal trees in the heart conditions. Heart conditions contains conflicting information are then removed by the Algorithm 3 *cutTree()* procedure.

The process can be logically divided into two steps: 1) enumerate all possible (not necessary plausible) heart conditions for each heart topology; and 2) eliminate heart conditions that violate physiological constraints. In practice these two steps are interleaved for optimization purpose. The rest of the section describes the algorithms in more detailed.

4.2 Enumeration of Heart Conditions

The enumeration of heart conditions is achieved by Algorithm 1 and Algorithm 2. Intuitively for each ambiguity encountered, create a new heart condition for each ambiguous situation. There are several sources of ambiguities:

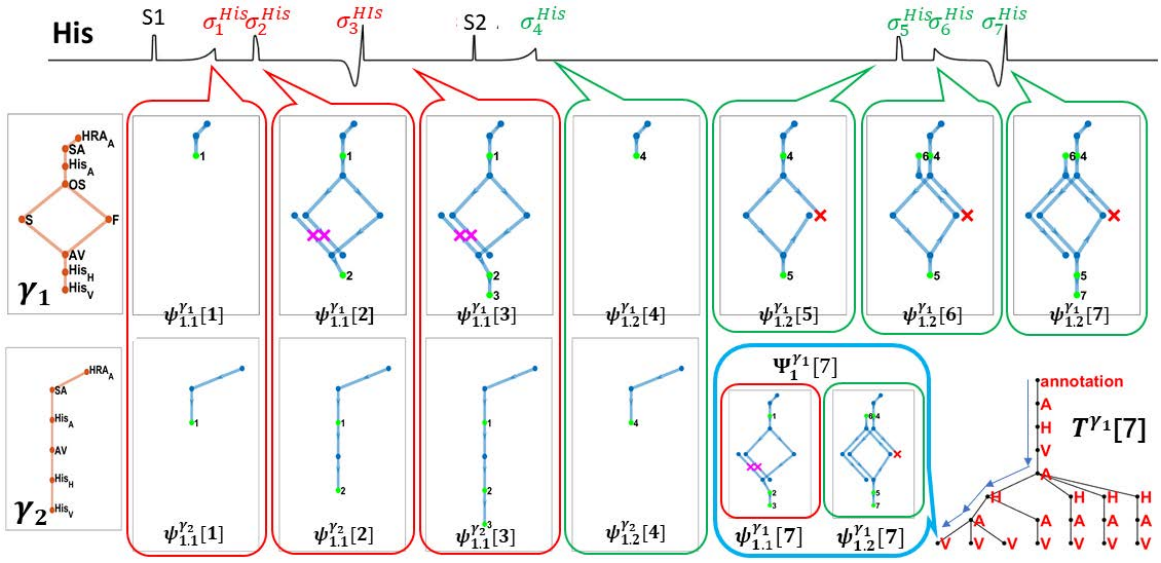

Figure 7: Traversal trees after each EGM observation. The drastically prolonged A-H interval caused elimination of γ_2 due to violations of historical information. The green vertices represent traversed v^O, the names of which are annotations for the σ_i.

4.2.1 Unknown Current State of the Heart Model. The patient's heart is a partially-observable system, which means that there may exist multiple heart state sequences that can explain historical observations. The state of the heart affects how electrical signals traverse the electrical conduction system. i.e. whether a timed automaton representing $v_i \in V$ is in its *ERP* location dictates whether electrical signals are blocked at v_i. To represent this uncertainty, the system creates two new heart conditions for 1) v_i is in *ERP*, and 2) v_i is not in *ERP*. In the first case the tree traverse will stop at v_i as the tissue blocked conduction, and in the second case the traverse will continue. This enumeration is achieved by adding new heart conditions at Line 18 and 19 in Algorithm 2.

4.2.2 Combinations of Traversal Trees. Each stimulus applied to the heart generates a traversal tree within the heart topology. Depending on the state of the heart, there can be multiple plausible traversal trees for each stimulus. Theoretically the number of traversal tree sets for the stimuli sequence $S = (s_1, s_2 \dots s_j)$ is equal to the size of the *Cartesian product* of all traversal tree sets $\Psi^{\gamma}_{n.s}$ for each stimulus s. In our system, all possible combinations of traversal trees are considered and each of the combination is represented by a heart condition. This enumeration is achieved at Line 9 in Algorithm 1.

4.2.3 Origin of the Signals. As discussed in Section 3.2, traversal trees in the same set may overlap in time. Therefore, ambiguity may exist about which tree an observable impulse belongs to. A heart condition is created for each of these ambiguous situations to capture the uncertainty. This enumeration is achieved by the for loop at Line 11 in Algorithm 1.

4.3 Elimination of Heart Conditions

Enumerated heart conditions that are 1) not be physiologically plausible, or 2) conflict with information from the new observation should be eliminated from consideration. There are physiological constraints that the heart conditions have to satisfy. In the system, we try to encode as few constraints as possible to maintain the generality of our approach.

4.3.1 Head-to-head Conduction Cancellation. Due to the refractory period of heart tissue, two electrical signals conducting towards each other on the same path will eventually collide and cancel each other. In our system, traversal on the same edge with opposite direction is detected and the node is marked as *conflict*, which will not be traversed further. This is achieved at Line 18 in Algorithm 2.

4.3.2 Consistency with Historical information. Each new observation may reveal new information regarding heart model parameters. As shown in Algorithm 3, we extract linear constraints on heart model parameters cp_n from new observations and combine them with cp in each suspected heart model. By doing linear programming, cp is either refined if there exists solutions, or the heart model is removed due to conflict information.

4.3.3 Prior Knowledge on Model Parameters. There exists physiological knowledge on parameter ranges related to certain heart conditions. Physicians sometimes use these knowledge to rule out suspected heart conditions. Similar to the physiological constraints, we aim to keep the amount of prior knowledge minimum in order to make less assumptions before the procedure. The physicians can manually rule out heart conditions from the system base on their experience.

4.4 Heart Model Parameter Identification

Identifying parameters for key tissue of the heart is essential during cardiac ablation. In each heart model, X represents the set of parameters for vertices and edges. cp is in form of $AX \leq B$, which represents linear constraints extracted from observations as well as

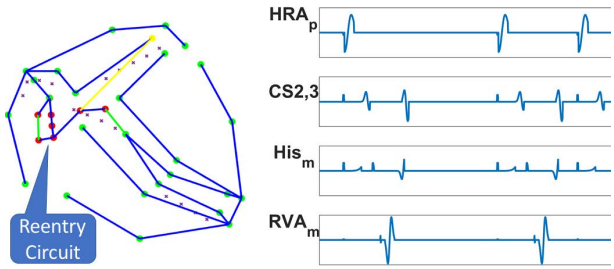

Figure 8: The VHM model for AVNRT by Jiang et.al[11]. The left panel shows the heart model with reentry circuit and its current state. The right panel shows synthetic EGM signals

prior knowledge. Linear programming is performed by the *linprog* function in the MATLAB Optimization Toolbox in $cutTree()$ on cp to update parameter ranges.

5 CASE STUDY

Reentry is the primary mechanism of Tachycardia and the most common target for cardiac ablation procedures [13]. Diagnosis is more challenging in reentry ablation due to the existence of circles in the heart topology. In this section, we demonstrate the capability of our clinical assist system to correctly diagnose Atrioventricular Nodal Reentry Tachycardia (AVNRT).

Patients with AVNRT have an accessory conduction pathway in the AV node, which forms a reentry circuit with the intrinsic pathway. During cardiac ablation procedure, physicians use programmed pacing to *induce* the reentry behavior, so that AVNRT can be confirmed and other arrhythmia with similar observations can be ruled out.

5.1 Virtual Patient and Synthetic EGMs

In this case study we use a virtual patient with AVNRT to demonstrate our system's capability to successfully identify the heart condition. Virtual patients are better suited in the early stage of this research as more extensive tests can be performed on a model compared to a patient, and we can obtain the ground truth of the heart condition. In [11], Jiang et.al developed the Virtual Heart Model (VHM) which can generate synthetic EGM signals for various heart conditions. The VHM can also respond to programmed pacing sequences applied by the physicians, which makes it a good model for preliminary evaluation of our system. In this project, we use VHM to represent the virtual patient with AVNRT (Fig. 8), and use synthetic EGM signals generated by the VHM as input to our clinical assist system. The parameters of the heart models are obtained from or optimized according to [13].

5.2 AVNRT Induction

In our virtual study, two heart topologies γ_1 and γ_2 are provided to the physicians before the procedure (Fig. 7), where γ_1 represents AVNRT with a reentry circuit and γ_2 represent a healthy heart. V^O for the His catheter v^{His_A}, v^{His_H} and v^{His_V}, and V^S for the HRA catheter v^{HRA_A} are included in the heart topologies. During the procedure, physician delivered stimuli sequences from v^{HRA_A} so that the heart exhibits different observable behaviors.

Fig. 7 shows the intermediate steps of heart condition update. In Section 4.1 we discussed system operation without introducing

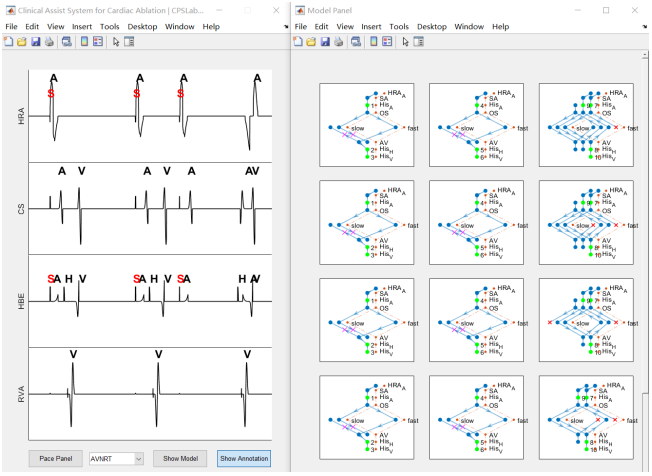

Figure 9: The interface for physicians. The left panel shows annotated EGM signals and the right panel visualizes traversal tree sets from suspected heart conditions.

the physiological context. The traversal tree set $\Psi_1^{\gamma_1}[7]$ under heart model $h_1^{\gamma_1}[7]$ matches the ground truth of how two stimuli conduct throughout the patient's heart. There are two conduction pathways in the AVNRT topology σ_1. From the visualization of $\psi_{1.1}^{\gamma_1}[3]$ we can see that the first stimulus $S1$ triggered conduction in both pathways. The signal arrived the exit of the reentry circuit via (F, AV). One branch triggered His_H and then His_V, which correspond to σ_2 and σ_3, while the other branch conducted through (AV, S) collide with conduction in the slower pathway (S, AV) and cancelled. From the visualization of $\psi_{1.2}^{\gamma_1}[7]$ we can see that the conduction of the second stimulus $S2$ is blocked at vertex v^F due to its long ERP. The signal conducted through the slower pathway and then started conduction within the reentry circuit, and AVNRT was induced.

5.3 Result Analysis

As shown in Fig. 7, our system was able to successfully identify AVNRT. During the procedure, physicians have real-time display of suspected heart conditions including heart topologies and traversal trees for each stimulus. EGM signals are also annotated for each heart condition (Fig. 9). As shown in Fig. 7, there are seven leaf vertices for $T^{\gamma_1}[7]$, and $h_1^{\gamma_1}[7]$ is one of the seven suspected heart conditions. The other six heart conditions have identical traversal trees with slightly different cp due to the limited observation so far.

Fig. 10 shows the number of heart conditions after updating the uncertainty tree for each observed EGM impulse. Without imposing physiological constraints, the amount of ambiguities during the procedure increases exponentially. R1-R5 correspond to different physiological knowledge encoded in our system, which was discussed in Section 4.2 and 4.3. With these physiological constraints imposed, our system was able to rule out physiologically implausible heart conditions.

In clinical setting, the seven EGM impulses occur within two seconds. In order to achieve real-time analysis, heart model update for each impulse has to finish within 100ms. The system is currently

implemented in MATLAB without any optimization. The average time to update one heart condition is around 170ms, and the computational time for updating heart conditions for each observed impulse is affected by the amount of suspected heart conditions. Efficiency can be improved by introducing parallelism during heart condition update.

6 RELATED WORK

Manufacturers of the cardiac ablation guidance systems have developed new algorithms to process the additional data by analysing and visualizing the timing correlations among new EGMs. However, the new algorithm still does not consider the ambiguities related to multiple suspected heart conditions. Clinical experiments of the new system only showed equivalent safety and effectiveness compared to traditional systems, with no advantage in terms of procedure time reduction [9].

There are also attempts to use heart model simulations for ablation guidance. Researchers at Johns Hopkins University have developed patient-specific heart models using MRI images of the heart. The heart models can be used to identify possible electrical conduction patterns with the presence of scar tissue, and propose optimal ablation cites [6]. However, these heart models can only be used for offline pre- and post-operation analysis, and can not address the ambiguity challenge during the procedure.

7 DISCUSSION AND FUTURE WORK

State estimation of partially-observable discrete-event systems is a challenging problem [2, 18]. With the system's parameters partially unknown as well, the problem is undecidable due to the large amount of ambiguous states and parameters. In this paper, we formalized the diagnosis problem during cardiac ablation as parameter identification and state estimation problems on timed automata heart models, and proposed a partial solution based on analysis of the heart model structure and domain knowledge. The proposed clinical assist system enumerates all possible heart conditions that can explain historical observations in terms of "digital twins" of the patient's heart. These digital twins are incrementally updated by information from new observations, which provide the physicians with interpretable visualization of the current understanding of the patient's heart.

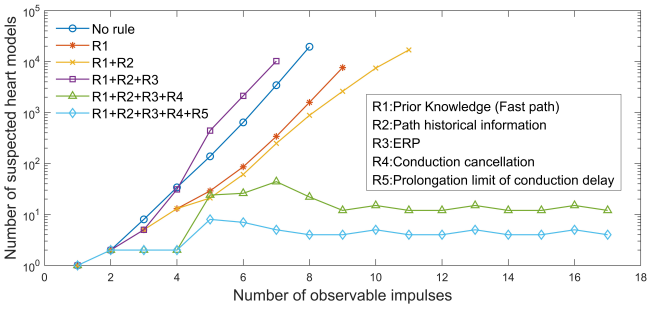

Figure 10: Number of heart conditions increases exponentially when all sources of ambiguity are considered. Illegal heart conditions are removed by imposing physiological constraints.

The next step of the project is to identify the optimal pacing sequences that can distinguish the suspected heart conditions. With suspected heart conditions explicitly enumerated, intuitively the problem can be formulated as *diagnosability* of certain states in the heart model. Diagnosability of discrete event system has been studied in the control community [19], which could provide inspirations for our problem.

We also plan to relax the assumptions we made during our preliminary evaluation. Ideally the system should be able to perform as well as the physicians in complex clinical cases.

REFERENCES

[1] R. Alur and D. L. Dill. 1994. A Theory of Timed Automata. *Theoretical Computer Science* 126 (1994), 183–235. Issue 2.

[2] F. Basile, M. P. Cabasino, and C. Seatzu. 2015. State Estimation and Fault Diagnosis of Labeled Time Petri Net Systems With Unobservable Transitions. *IEEE Trans. Automat. Control* 60, 4 (2015), 997–1009. https://doi.org/10.1109/TAC.2014.2363916

[3] Deepak Bhakta and John M Miller. 2008. Principles of Electroanatomic Mapping. *Indian Pacing Electrophysiol J* 8, 1 (2008), 32–50.

[4] Jui-Kun Chiang, Hsueh-Hsin Kao, and Yee-Hsin Kao. 2017. Association of Paroxysmal Supraventricular Tachycardia with Ischemic Stroke: A National Case-Control Study. *Journal of Stroke and Cerebrovascular Diseases* 26, 7 (2017), 1493 – 1499.

[5] Sumeet S Chugh, Rasmus Havmoeller, Kumar Narayanan, David Singh, Michiel Rienstra, Emelia J Benjamin, Richard F Gillum, Young-Hoon Kim, John H McAnulty Jr, Zhi-Jie Zheng, et al. 2014. Worldwide epidemiology of atrial fibrillation: a Global Burden of Disease 2010 Study. *Circulation* 129, 8 (2014), 837–847.

[6] D Deng, A Prakosa, P Nikolov, and NA Trayanova. 2019. Sensitivity of Ablation Targets Prediction to Electrophysiological Parameter Variability in Image-Based Computational Models of Ventricular Tachycardia in Post-infarction Patients. *Front Physiol* 10, 628 (2019).

[7] Abhishek Deshmukh, Nileshkumar J. Patel, Sadip Pant, Neeraj Shah, Ankit Chothani, Kathan Mehta, Peeyush Grover, Vikas Singh, Srikanth Vallurupalli, Ghanshyambhai T. Savani, Apurva Badheka, Tushar Tuliani, Kaustubh Dabhadkar, George Dibu, Y. Madhu Reddy, Asif Sewani, Marcin Kowalski, Raul Mitrani, Hakan Paydak, and Juan F. Viles-Gonzalez. 2013. In-Hospital Complications Associated With Catheter Ablation of Atrial Fibrillation in the United States Between 2000 and 2010. *Circulation* 128, 19 (2013), 2104–2112.

[8] Tao F, Cheng J, and Qi Q et al. 2018. Digital twin-driven product design, manufacturing and service with big data. *Int J Adv Manuf Technol* 94 (2018), 3563. Issue 9.

[9] Hindricks G, Weiner S, and McElderry T et al. 2019. Acute safety, effectiveness, and real-world clinical usage of ultra-high density mapping for ablation of cardiac arrhythmias: results of the TRUE HD study. *Europace* 21 (2019), 655-661. Issue 4.

[10] Zhihao Jiang, Miroslav Pajic, Rajeev Alur, and Rahul Mangharam. 2014. Closed-loop verification of medical devices with model abstraction and refinement. *International Journal on Software Tools for Technology Transfer* 16, 2 (01 Apr 2014), 191–213.

[11] Z. Jiang, M. Pajic, and R. Mangharam. 2012. Cyber–Physical Modeling of Implantable Cardiac Medical Devices. *Proc. IEEE* 100, 1 (2012), 122–137.

[12] RM John and W Stevenson. 2018. *Electrophysiology Approaches for Ventricular Tachycardia.* Elsevier.

[13] Mark E Josephson. 2015. *Josephson's clinical cardiac electrophysiology.* Lippincott Williams & Wilkins.

[14] Kneeland, Patrick P, and Margaret C Fang. 2009. Trends in catheter ablation for atrial fibrillation in the United States. *Journal of hospital medicine* 4, 7 (2009), E1–5.

[15] ROBERT J. MYERBURG. 1986. Epidemiology of Ventricular Tachycardia/Ventricular Fibrillation and Sudden Cardiac Death. *Pacing and Clinical Electrophysiology* 9, 6 (1986), 1334–1338.

[16] Matthew R Reynolds, Joshua Walczak, Sarah A White, David J Cohen, and David J Wilber. 2010. Improvements in symptoms and quality of life in patients with paroxysmal atrial fibrillation treated with radiofrequency catheter ablation versus antiarrhythmic drugs. *Circulation: Cardiovascular Quality and Outcomes* 3, 6 (2010), 615–623.

[17] Peter Spector. 2013. Principles of cardiac electric propagation and their implications for re-entrant arrhythmias. *Circulation: Arrhythmia and Electrophysiology* 6, 3 (2013), 655–661.

[18] Xiang Yin. 2019. Estimation and Verification of Partially-Observed Discrete-Event Systems. *CoRR* abs/1903.11413 (2019). arXiv:1903.11413 http://arxiv.org/abs/1903.11413

[19] J. Zaytoon and S. Lafortune. 2013. Overview of fault diagnosis methods for Discrete Event Systems. *Annual Reviews in Control* 37, 2 (2013), 308 – 320.

APPENDIX

Algorithm 1 Analyze EGM

Input: Uncertainty tree $T^{\gamma}[k-1]$, sequence of paced stimuli $S = (s_p^j | p \in \mathbb{N}, v_j^S \in V^S)$, heart topology γ
Output: updated $T^{\gamma}[k]$
procedure $T^{\gamma}[k]$ = AnalyzeEGM($S, T^{\gamma}[k-1]$)
  for $h_i^{\gamma}[k-1]$ in leaves of $T^{\gamma}[k-1]$ **do**
    ▷ Find all possible heart models that can explain σ_k
    $tempModels \leftarrow []$
    for $s = 1$ to the number of S **do**
      ▷ Enumerate all possible traversal tree sets
      $tempModels \leftarrow tempModels \times$ TpTraverseIter($\gamma, v_j^S, h_i^{\gamma}.\psi_{p.s}^{\gamma}[k-1]$)
    for $q \leftarrow 1$ to the number of traversal tree sets in $tempModels$ **do**
      for $s \leftarrow 1$ to the number of S **do**
        $annotNodes \leftarrow$ all v^O in $\psi_{q.s}^{\gamma}[k]$ that can explain the current observation σ_k
        $annots \leftarrow$ The names of $annotNodes$
        $cp \leftarrow$ linear constraints on parameters of γ
        for m in 1 to length of $annots$ **do**
          ▷ Create heart models for each annotation
          Add new heart model $h_m^{\gamma}[k]$ in $T^{\gamma}[k]$ with edge $(h_i^{\gamma}[k-1], h_m^{\gamma}[k])$
          $h_m^{\gamma}[k].annot \leftarrow annots[m]$
          $h_m^{\gamma}[k].cp \leftarrow h_i^{\gamma}[k-1].cp \cup cp[m]$
          mark $annotNodes[m]$ in $h_m^{\gamma}[k].\psi_{m.s}^{\gamma}[k]$ as annotated
          $h_m^{\gamma}[k].\Psi_k^{\gamma}[k] \leftarrow \Psi_q^{\gamma}[k]$

Algorithm 2 Topology Traversal

Input: heart topology γ, the vertex that receives the sth stimulus $v^S \in V^S$, a traversal tree ψ^{γ}
Output: traversal trees for the sth stimulus $\Psi_{n.s}^{\gamma} = (\psi_{1.s}^{\gamma}, \psi_{2.s}^{\gamma} \cdots \psi_{n.s}^{\gamma})$
procedure $\Psi_{n.s}^{\gamma}$ = TpTraverseIter($\gamma, v^S, \psi^{\gamma}$)
  if $\psi^{\gamma} = \emptyset$, $\psi^{\gamma} \leftarrow v^S$
  $ExpandableNodes \leftarrow [\,]$
  for v_1 in leaves of ψ^{γ} **do**
    ▷ Find expandable vertices
    if $(v_1 \in V \setminus V^O) \wedge (v_1$ not marked as ERP$) \wedge (v_1$ not marked as conflict$) \vee (v_1 \in V^O \wedge v_1$ is marked as annotated) **then**
      Add v_1 to list $ExpandableNodes$.
  $\Psi_{n.s}^{\gamma} \leftarrow \psi^{\gamma}$
  if $ExpandableNodes = \emptyset$ **then**
    return $\Psi_{n.s}^{\gamma}$
  for v_i in list $ExpandableNodes$ **do**
    ▷ Expand trees for one step
    Find vertices $V^n = \{v_j^n\}$ with edge (v_i, v_j^n) in γ
    for ψ_k^{γ} in $\Psi_{n.s}^{\gamma}$ **do**
      Add vertices V^n and edges (v_i, v_j^n) in ψ_k^{γ}
      $\psi_{ERP}^{\gamma} \leftarrow \psi_k^{\gamma}$, mark v_j^n as ERP in ψ_{ERP}^{γ}
      $\Psi_{n.s}^{\gamma} \leftarrow \Psi_{n.s}^{\gamma} \cup \psi_{ERP}^{\gamma}$
      if there exists both (v_i, v_j^n) and (v_j^n, v_i) in ψ_k^{γ} **then**
        mark v_i as conflict
  $temp\_Tset \leftarrow [\,]$
  for ψ_m^{γ} in $\Psi_{n.s}^{\gamma}$ **do**
    $temp\_Tset \leftarrow temp\_Tset \cup$ TpTraverseIter($\gamma, v^S, \psi_m^{\gamma}$)
    ▷ Expand until no expandable vertices available
  $\Psi_{n.s}^{\gamma} \leftarrow temp\_Tset$

Algorithm 3 Cut Uncertainty Tree

procedure cutTree(T^{γ})
  for h_i^{γ} in leaves of T^{γ} **do**
    Extract cp_n from EGMs regarding $h_i^{\gamma}.\gamma$
    Combine the linear constraints $h_i^{\gamma}.cp \cup cp_n$
    if $h_i^{\gamma}.cp \cup cp_n$ have no solution by linear programming **then**
      Remove h_i^{γ} from T^{γ}